

Rapid Commun. Mass Spectrom. 2015, 29, 1019–1024
(wileyonlinelibrary.com) DOI: 10.1002/rcm.7191

Resolution pattern for mass spectrometry imaging

Stephan R. Fagerer¹, Andreas Römpf², Konstantins Jefimovs³, Rolf Brönnimann³, Gerd Hayenga⁴, Robert F. Steinhoff¹, Jasmin Krismer¹, Martin Pabst¹, Alfredo J. Ibáñez¹ and Renato Zenobi^{1*}

¹ETH Zürich, Department of Chemistry and Applied Biosciences, 8093 Zürich, Switzerland

²University of Giessen, Institute of Inorganic and Analytical Chemistry, Schubertstrasse 60, D-35392 Giessen, Germany

³EMPA (Swiss Federal Laboratories for Material Science and Technology), Überlandstrasse 129, Dübendorf, Switzerland

⁴Sigma-Aldrich Chemie GmbH, Industriestrasse 25, Buchs (SG), Switzerland

RATIONALE: Up to now, there is no 'gold standard' for determining the resolution of a mass spectrometry imaging (MSI) setup (comprising the instrument, the sample preparation, the sample and the instrument settings). A standard sample in combination with a standard protocol to define the MSI resolution would be desirable in order to compare the setups of different laboratories, and as a regular quality control/performance check.

METHODS: Microstructured resolution patterns were fabricated that can be used to determine the spatial resolution in MSI experiments, down to the range of a few μm . Two different strategies were employed, one where the resolution pattern is laser machined into a thin metal foil, which can be placed over a sample to be imaged, and a second one where hydrophilic grooves are machined into an omniphobic coating covering the surface of an indium tin oxide covered glass slide. When dragging a sample solution over the slide's surface, the sample is automatically retained in the hydrophilic grooves, but repelled by the omniphobic coating.

RESULTS: The technology was tested on a commercial matrix-assisted laser desorption/ionization (MALDI) imaging instrument, and a spatial resolution in the vicinity of 50 μm was determined. The finest features of the microstructured resolution patterns are compatible with the best spatial resolution of MALDI imaging systems available to date.

CONCLUSIONS: The use of metal resolution grids or glass slides with hydrophilic/hydrophobic structures is suitable for the convenient determination of the resolution limit of the MALDI imaging instrument as determined by its hardware. These structures are straightforward both to produce and to use. Copyright © 2015 John Wiley & Sons, Ltd.

Mass spectrometry imaging (MSI) has emerged as a powerful tool to visualize the distribution of biomolecules in thin tissue sections. It has been successfully used for lipids,^[1] peptides,^[2] proteins, but also drugs.^[3] Sensitivity and spatial resolution are the two most important parameters defining the imaging capabilities of MSI. While the first is vital for the ability to detect target analytes even in low concentrations and/or in complex biological matrices, the latter is important to discern even fine structures on tissues. The best spatial resolution that a matrix-assisted laser desorption/ionization (MALDI) instrument is capable of is determined by a number of factors. The most important ones are the size of the laser focus and the sample (e.g. tissue) preparation. However, the minimum sample stage motion increment may also play a role in this respect. Typically, MSI experiments are performed at a pixel size of 50 to 200 μm . However, recent advances in instrumentation have made much higher resolution experiments possible. Imaging of phospholipids and other compound classes has been performed at a pixel size between

3 and 5 μm .^[4,5] Moreover, MALDI images with pixel size as low as 1 μm have been obtained.^[6–8] With modified commercial systems a resolution of 10 μm was reported for lipids^[9] and proteins.^[10] Another approach is the microscope mode that enables pixel sizes much smaller than the laser beam diameter.^[11]

Up to now, there is no 'gold standard' for determining the resolution of an imaging setup (comprised of the instrument, the sample preparation, the sample and the instrument settings). A standard sample in combination with a standard protocol to define the MSI resolution, however, would be desirable in order to compare the setups of different laboratories, and as a regular quality control/performance check. Conventional approaches to evaluate the spatial resolution often involve biological structures with features of known dimensions (from microscopic analysis). However, such structures are sample dependent and unique, and comparison is therefore more complicated. In contrast, transmission electron microscopy (TEM) grids with metal bars down to a thickness of a few microns are mass-produced and can be easily acquired by any lab.^[12] While TEM grids are readily available and therefore suitable for comparative studies, the features are very simple, with only uniform structural elements. A TEM grid may be used to demonstrate that the resolving capabilities of a given

* Correspondence to: R. Zenobi, ETH Zürich, Department of Chemistry and Applied Biosciences, 8093 Zürich, Switzerland. E-mail: zenobi@org.chem.ethz.ch

system surpass a certain threshold, but will typically not allow one to determine the best resolving capability of an imaging system.

In this article, we present two convenient strategies to rapidly evaluate the spatial resolution that can be reached with a MSI instrument. Both methods rely on a resolution pattern like those found on the so-called Koren test charts, which are used to determine the resolution capabilities of cameras and lenses. Similar experiments have been performed using organic periodic gratings and inkjet-printed patterns.^[13,14] In contrast, our strategy was to employ patterned tungsten grids and pre-structured polysilazane-coated indium-tin oxide (ITO) glass slides, which allow for experiments that can be reproduced many times without much effort, even in inter-laboratory comparison studies, e.g., by distribution of identical copies or by shipping the grids/slits, which is possible because these structures are not destroyed by the measurements. For both, a series of parallel lines of sample is generated with an increasing density from one side to the other. In addition, the line width decreases in the same direction. The spatial resolution of an MSI experiment is reached once two adjacent lines cannot be distinguished any longer.

EXPERIMENTAL

Chemicals

The MALDI matrices, 9-aminoacridine and α -cyano-4-hydroxycinnamic acid, and methanol (HPLC grade) and acetonitrile (HPLC grade) were purchased from Sigma-Aldrich (Buchs, Switzerland). Angiotensin II was bought from Bachem (Bubendorf, Switzerland). Tungsten foils (20- μ m thickness) were from Goodfellow (Huntingdon, UK). ITO/glass slides were obtained from Sigma-Aldrich and coated with an approximately 1–5 μ m thick layer of polysilazane.

Patterning of tungsten and polysilazane ITO slides

Patterning of the tungsten grids as well as structuring of the polysilazane-coated ITO slides was performed with a picosecond scanning laser ablation system, as described in Pabst *et al.*^[15] and Urban *et al.*^[16] The quality of the grids and structures was evaluated using a Nikon microscope.

Sample preparation for the method using a tungsten grid

(i) 9-Aminoacridine (10 mg/mL in MeOH, 0.5 μ L) was spotted onto a brushed stainless steel plate and dried at room temperature. (ii) Using a thin layer preparation technique, α -cyano-4-hydroxycinnamic acid (10 mg/mL, 50% acetonitrile, 0.1% trifluoroacetic acid (TFA), 4 μ L) and angiotensin II (240 μ M in H₂O, 4 μ L) were sequentially spotted onto a custom-made brushed stainless steel MALDI plate with squares milled into that plate to retain the matrix/sample solution (5 mm side length). The matrix/sample solution was spotted at 80 °C using a heating plate so as to speed up the drying process, which yields smaller and more uniform crystals. (iii) 500 μ L of a 1:1 mix of α -cyano-4-hydroxycinnamic acid (10 mg/mL, 50% acetonitrile, 0.1% TFA) and angiotensin II (240 μ M in H₂O) was sprayed onto a stainless steel plate using an airbrush (1 bar pressure).

Once the sample had dried the target was fixed onto the support using green masking tape (Kapton, Torrance, CA, USA), which contains a glue that does not outgas and is therefore compatible with the vacuum of the mass spectrometer. The tape was applied to all four edges to ensure that the grid was flat.

Sample preparation for the method using an ITO-coated glass slide

Matrix application onto polysilazane-coated ITO glass slides was carried out by dragging a 5- μ L-sized droplet along the patterned surface (Fig. 1(B)). Due to the hydrophilic grooves of the grid, which were generated by laser ablation, a discrete volume of matrix solution is trapped in each. Excess volume from sample aliquoting was removed, and the slide was then left for a few minutes in ambient atmosphere to dry. The same procedure was followed once for a 2 μ M *fluorescein* solution (in 50% acetonitrile) in order to allow orthogonal fluorescence readout by a LS400 scanner (Tecan, Zurich, Switzerland). For the mass spectrometry experiments, the ITO slide was mounted on a metal target carrier (AB Sciex, Framingham, MA, USA) by using a mask and copper tape as included in the LaserBio Labs™ Mass Spectrometry Imaging Starter Kit (AB Sciex).

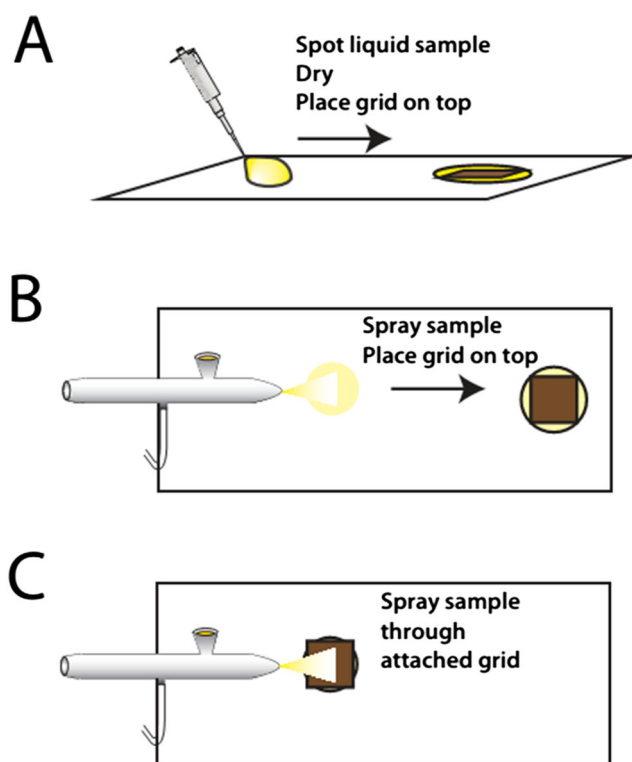


Figure 1. Three different ways to apply MALDI matrix to the target in a homogeneous way when using the tungsten grid resolution pattern. (A) The matrix solution is pipetted onto the metal target, followed by covering the MALDI sample with the grid. (B) An airbrush is used to spray the MALDI matrix solution onto the target, followed by covering the MALDI sample with the grid. (C) The resolution grid is placed onto the metal target and the MALDI matrix is sprayed with an airbrush.

Mass spectrometry

All experiments not involving tissue were performed on an AB Sciex 5800 MALDI ToF/ToF instrument. The Nd:YLiF laser (349 nm) had a focal diameter of approx. 30 μm , and was operated at a repetition rate of 1 kHz. Using the AB Sciex spot set editor a rectangular raster pattern was created with circular spots with a diameter and center-to-center spacing of 15 μm . At each position 100 subspectra were collected and averaged. The laser energy was set to 3900 (arbitrary units).

Data processing

The spectra were exported to t2d files and converted to txt format using a Java applet ("Peak list conversion tool" by Jayson Falkner, which was available under www.proteomecommons.com in 2011, but has since been abandoned). A MATLAB script written in-house was used to extract peak intensities and create a heat map (location represented by x and y coordinates and ion intensity displayed as a color code).

Determination of the resolution limit

An objective criterion for the resolution limit was defined, to allow for unbiased analysis of the imaging results. When analyzing two-dimensional line plots, the limit is met once the background signal, i.e., the valley between two lines, does not fall below a signal height larger than the average background (of the left half of the line plot, where it is well-defined) with the addition of three times the standard deviation of the said background. It should be noted that other, rather complex approaches for analyzing imaging systems exist, for instance the calculation of modulation transfer functions.^[14]

RESULTS AND DISCUSSION

When using the tungsten grid, evaluating the spatial resolution of a MALDI imaging setup involves three steps: (i) applying a suitable sample onto the sample support in a highly uniform fashion, (ii) positioning the grid over the sample, and (iii) analyzing the sample via a MALDI imaging protocol. The first step is critical, since an inhomogeneous deposition of material may result in an incomplete image with lines missing. We tested different modes of applying the matrix, namely spotting the sample onto a metal target followed by covering the MALDI sample with the grid (Fig. 1(A)), spraying the sample with an airbrush onto a metal target followed by covering the MALDI sample with the grid (Fig. 1(B)), or spraying the sample onto the target while using the grid as a spraying mask (Fig. 1(C)). We found that the first two methods of application produce homogenous MALDI images, whereas the third method is not suitable due to crystals clogging the slits. The most suitable deposition method also depends on the matrix/solvent system. Very volatile solvent mixtures, such as acetone/water, which were used for 9AA lend themselves favorably to liquid deposition using a pipette, since the fast evaporation of low volumes (we used 2 μL) does not allow for the formation of long crystals. On the other hand, we preferred spraying DHB dissolved in acetonitrile/water using a paint brush gun.

We now discuss the use of the resolution grid that features lines with continuously shrinking distances (Fig. 2). Figure 2(C) shows a MALDI image resulting from measuring a homogenous layer of 9-aminoacridine ($[M+H]^+$ ion at m/z 195) applied by wet spotting with a tungsten grid (Figs. 2(A) and 2(B), respectively) placed on top. We opted for a gap range of 100 down to 4 μm , which is in the same range as MALDI imaging setups with the currently highest available spatial resolution.^[5,17] At the left side of the grid (between the lines with 100 to 60 μm gaps) we chose to use a line interval of 10 μm , whereas at the right end (60 μm and smaller gaps) the interval is significantly narrower, i.e. 2 μm . In principle, modern MALDI mass spectrometers have relatively uniform laser beam profiles in the x- and y-directions. However, this is often not true for older instruments. In such cases, the grid may be turned by 90° after the first experiment and the resolution in the perpendicular direction can be determined subsequently. This design was chosen since most commercially available MALDI mass spectrometers are equipped with an Nd:YAG laser or N₂ laser with spot sizes between 20 and 50 μm in diameter and the grid offers a smaller interval in this region of interest. It should be noted that for a Gaussian laser spot profile, the spot size is dependent on the laser energy.^[18–20] As a result, the most meaningful resolution test results are achieved when the choice of matrix, the mode of matrix application and the

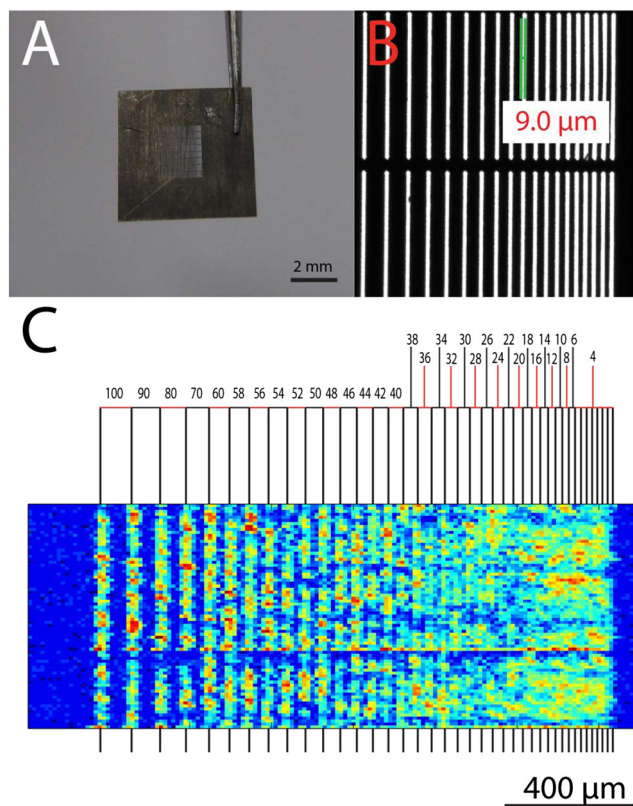


Figure 2. (A) Photographic image of a tungsten resolution pattern. (B) Optical micrograph of the top right corner of the pattern, showing a detailed view of said resolution pattern. (C) MALDI-MS image of 9-aminoacridine (m/z 195) at 15 μm pixel size in positive mode recorded with a resolution grid placed on top of the matrix. The resolution grid features 9 μm slits with decreasing distance.

laser energy setting are identical to those that are also used for the (prospective) imaging experiment. Although the lines are clearly visible, which means that the ions pass successfully from the sample through the grid to the detector, most lines appear jagged or broken. This may stem from either minor inhomogeneities in the sample/matrix application. Nonetheless, the spatial resolution may still be determined without any problem. The horizontal gap that can be seen in Fig. 2(C) (and also in Fig. 3(C)) stems from a connector piece in the grid, which was introduced for stability reasons. In Fig. 2(C), individual lines can be distinguished until a gap distance of 48 μm according to our resolution limit criterion. This spatial resolution for the AB Sciex 5800 is in agreement with that reported for other commercial MALDI-TOF mass spectrometers in routine operation.^[21] If the MALDI instrument has a different resolution in the x- and y-directions, the grid may be turned by 90°.

A more accurate estimation of the spatial resolution is possible if the width of the bridges is equal to that of the lines (Fig. 3). Checking the spatial resolution on both the 'positive' (slits) and 'negative' (gaps) pattern is beneficial in case the nature of the sample or its application may create artifacts (e.g. line broadening by 'bleeding' of the sample). Figure 3(C) shows a MALDI image resulting from measuring a homogeneous layer of angiotensin II ($[\text{M}+\text{H}]^+$ ion at m/z 1046)

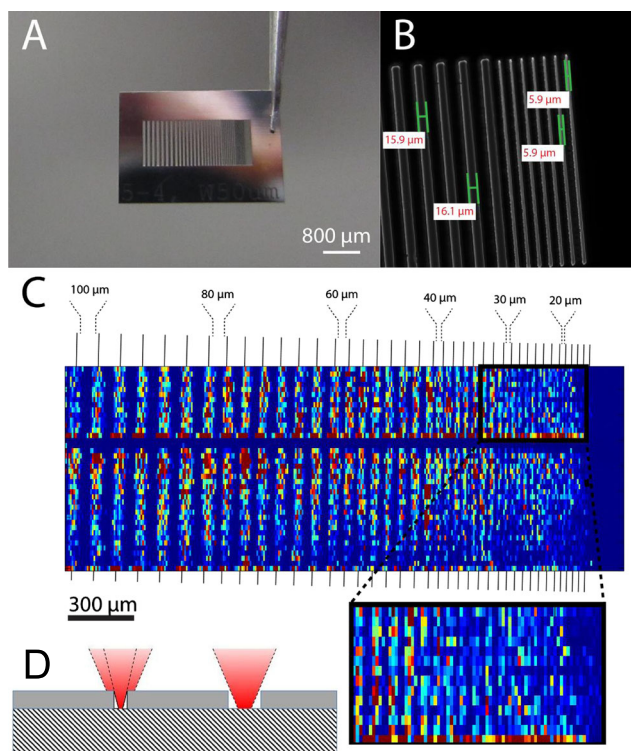


Figure 3. (A) Photographic image of a tungsten resolution pattern. (B) Optical micrograph, showing a detail of the resolution pattern. The resolution grid features slits and gaps with an almost identical width. (C) MALDI-MS image of angiotensin II (m/z 1046) at 15 μm pixel size in positive mode, with a resolution grid placed on top of the sample (matrix: α -cyano-4-hydroxycinnamic acid). (D) Depending on the aspect ratio of a groove in the resolution pattern, the laser beam may be clipped, resulting in signal loss.

premixed with α -cyano-4-hydroxycinnamic acid, which was applied by spraying. The tungsten grid with slits and bridges of equal width was laid on top (Figs. 3(A) and 3(B)). Here, we chose a design with slit/gap widths of 100-80-60-40-30-20 μm , each slit width being represented six times and each gap width being represented five times. We chose larger intervals than those in the embodiment shown in Fig. 3, i.e., 10 and 2 μm , since the laser parameters for each slit width must be tediously optimized for the picosecond laser ablation process. We also note that depending on the aspect ratio of a groove in the resolution pattern, the laser beam may be clipped, resulting in loss of MS ion signal, because not the entire beam energy arrives at the focus (left-hand part of Fig. 3(D)). For 20- μm -thick tungsten foils, this will for many MSI systems result in a practical limitation for using the resolution pattern for very fine features, of the order of approx. 5 μm .

The MALDI image of angiotensin (Fig. 3(C)) features a better S/N ratio than that recorded when using 9-aminoacridine (cf. Fig. 2(C), which may be because there is less background interference in the high m/z range (m/z 1046 for angiotensin) than there is in the low m/z range (m/z 195 for 9-aminoacridine). In agreement with the spatial resolution value determined above, the slits/gaps at 60 μm width are readily discernible and the resolution limit is met at the 40 μm mark (Supplementary Fig. S1, see Supporting Information). In addition to a quick sample preparation (covering the applied sample with a tungsten grid) the main benefit of either method is that the grid is reusable and may be cleaned with many different solvents. Furthermore, the grid may be mass produced with high accuracy and reproducibility if desired. This would be especially important if the MALDI imaging community were to adopt this tungsten resolution grid as a routine way for demonstrating the resolution capabilities of a setup.

We also tested a second strategy by employing a variation of our previously published Microarrays for Mass Spectrometry (MAMS) technology.^[15,16] A conductive glass slide was coated with polysilazane, an omniphobic transparent material. Figure 4 shows how the sample is applied in the case of the structured polysilazane-coated ITO slides. A droplet containing a mixed solution of sample and matrix is simply dragged over the surface of the array using a hydrophilic edge. During this, small sample/matrix volumes are trapped in the hydrophilic grooves. The pattern shown in Figs. 5 and 6 was then created by removing the polysilazane and ITO where the slits would have been in the tungsten resolution grid. These lines are hydrophilic as opposed to the surrounding polysilazane. If a

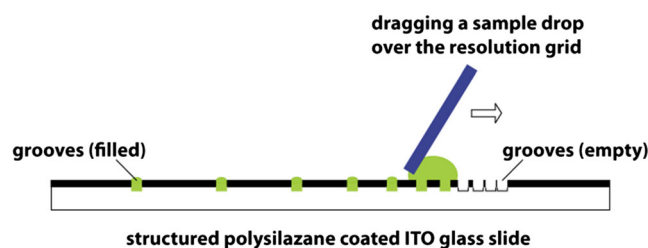


Figure 4. Application of structured polysilazane-coated ITO slides: Sample/matrix is applied through an aliquoting process. A droplet is simply dragged over the array using a hydrophilic edge and small sample/matrix volumes are trapped in the hydrophilic grooves.

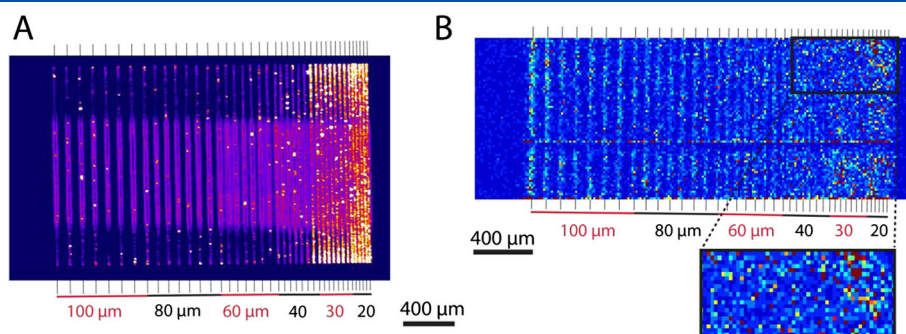


Figure 5. (A) Fluorescence image of a solution of fluorescein, aliquoted onto a MAMS chip with a pattern of hydrophilic lines surrounded by an omniphobic coating. (B) MALDI-MS image of a solution of 9-aminoacridine (m/z 195) aliquoted onto the MAMS chip used in (A), recorded in positive mode at $15\ \mu\text{m}$ pixel size. The numbers in red and black on the bottom of each part indicate the spacing between adjacent lanes.

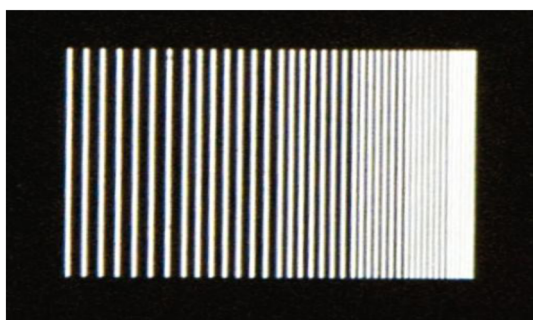


Figure 6. Image of the polysilazane (black colored) coated ITO slide, as used above for the fluorescence or MALDI-MS image, respectively.

sample is dragged across these lines, it selectively fills out the lines but does not stick anywhere between those lines (Fig. 4). This aliquoting effect was demonstrated by dragging $10\ \mu\text{L}$ of a fluorescein solution (in 50% acetonitrile) at a concentration of $2\ \mu\text{M}$ across the line pattern and recording a fluorescent image of the chip using the Tecan scanner (Fig. 5(A)). Indeed, there is little to no fluorescence signal detected between the said lines. It was observed that there is a brighter stripe in the center of the lines, which may be a result of the drying process, where the liquid tends to retract towards the inner part of the line.

Furthermore, the lines with a gap distance of $4\ \mu\text{m}$ seem to feature a much brighter fluorescence signal than the others, which may stem from the fact that the lines are so close together that a droplet is retained above the whole segment and that liquid is only aliquoted into the lines during the volume reduction of the drying process. The aliquoting process was then repeated with a solution of 9-aminoacridine and a MALDI image was recorded (Fig. 5(B)). While the S/N ratio is not as low as is shown for Fig. 3(C), the lines are clearly visible and have fewer interruptions than the preparation shown in that figure. The advantage of this method over using the tungsten grid is that the sample preparation is very fast and straightforward, compared, for instance, with spraying protocols. On the other hand, the aliquoting process by dragging a droplet does not work for highly viscous samples (this can be the case for physiological fluids), or solutions containing a very high fraction of organic solvent.

CONCLUSIONS

There is currently no widely accepted method available to determine the spatial resolution of a MALDI imaging setup, which is necessary for comparing different setups. The presented tungsten resolution grids and patterned ITO-coated slides are a step towards this goal by creating a selected ion image with a line pattern featuring a shrinking line distance from left to right (or vice versa) down to $4\ \mu\text{m}$, which is in the range of the highest spatial resolution reached with current MALDI imaging setups. The spatial resolution is reached when two lines cannot be distinguished any more. The fabrication of these tungsten grids may be easily scaled up and is very reproducible. Such a resolution grid can provide a convenient and reproducible way of evaluating the spatial resolution of a given instrumental setup, either for comparison with other laboratories or for evaluating performance over time.

Acknowledgements

This project was co-financed by the Swiss KTI (Kommission für Technologie und Innovation), Grant No. 13123.1 PFNM-NM. We also thank AB Sciex for the loan of an ABI 5800 MALDI ToF MS instrument. We also thank Fabian Wahl, Rudolf Köhling and Jens Boertz, from Sigma Aldrich, for their valuable input in developing the microarray technology.

REFERENCES

- [1] S. N. Jackson, H. Y. J. Wang, A. S. Woods. In situ structural characterization of phosphatidylcholines in brain tissue using MALDI-MS/MS. *J. Am. Soc. Mass Spectrom.* **2005**, *16*, 2052.
- [2] G. D. Brand, F. C. Krause, L. P. Silva, J. R. S. A. Leite, J. A. T. Melo, M. V. Prates, J. B. Pesquero, E. L. Santos, C. R. Nakaie, C. M. Costa-Neto, C. Bloch. Bradykinin-related peptides from *Phyllomedusa hypochondrialis*. *Peptides* **2006**, *27*, 2137.
- [3] Y. Hsieh, R. Casale, E. Fukuda, J. W. Chen, I. Knemeyer, J. Wingate, R. Morrison, W. Korfmacher. Matrix-assisted laser desorption/ionization imaging mass spectrometry for direct measurement of clozapine in rat brain tissue. *Rapid Commun. Mass Spectrom.* **2006**, *20*, 965.

- [4] A. Römpp, S. Guenther, Y. Schober, O. Schulz, Z. Takats, W. Kummer, B. Spengler. Histology by mass spectrometry: Label-free tissue characterization obtained from high-accuracy bioanalytical imaging. *Angew. Chem. Int. Ed.* **2010**, *49*, 3834.
- [5] A. Römpp, B. Spengler. Mass spectrometry imaging with high resolution in mass and space. *Histochem. Cell Biol.* **2013**, *139*, 759.
- [6] B. Spengler, M. Hubert, R. Kaufmann, in *Proc. 42nd ASMS Conf. Mass Spectrometry and Allied Topics*, Chicago, Illinois, **1994**, p. 1041.
- [7] B. Spengler, M. Hubert. Scanning microprobe matrix-assisted laser desorption/ionization (SMALDI) mass spectrometry: Instrumentation for sub-micrometer resolved LDI and MALDI surface analysis. *J. Am. Soc. Mass Spectrom.* **2002**, *13*, 735.
- [8] W. Bouschen, O. Schulz, D. Eikel, B. Spengler. Matrix vapor deposition/recrystallization and dedicated spray preparation for high-resolution scanning microprobe matrix-assisted laser desorption/ionization imaging mass spectrometry (SMALDI-MS) of tissue and single cells. *Rapid Commun. Mass Spectrom.* **2010**, *24*, 355.
- [9] A. Thomas, J. L. Charbonneau, E. Fournaise, P. Chaurand. Sublimation of new matrix candidates for high spatial resolution imaging mass spectrometry of lipids: Enhanced information in both positive and negative polarities after 1,5-diaminonaphthalene deposition. *Anal. Chem.* **2012**, *84*, 2048.
- [10] J. Yang, R. M. Caprioli. Matrix sublimation/recrystallization for imaging proteins by mass spectrometry at high spatial resolution. *Anal. Chem.* **2011**, *83*, 5728.
- [11] J. H. Jungmann, R. M. Heeren. Emerging technologies in mass spectrometry imaging. *J. Proteomics* **2012**, *75*, 5077.
- [12] M. Koestler, D. Kirsch, A. Hester, A. Leisner, S. Guenther, B. Spengler. A high-resolution scanning microprobe matrix-assisted laser desorption/ionization ion source for imaging analysis on an ion trap/Fourier transform ion cyclotron resonance mass spectrometer. *Rapid Commun. Mass Spectrom.* **2008**, *22*, 3275.
- [13] L. Qiao, E. Tobolkina, A. Lesch, A. Bondarenko, X. Zhong, B. Liu, H. Pick, H. Vogel, H. H. Girault. Electrostatic spray ionization mass spectrometry imaging. *Anal. Chem.* **2014**, *86*, 2033.
- [14] M. K. Passarelli, J. Wang, A. S. Mohammadi, R. Trouillon, I. Gilmore, A. G. Ewing. Development of an organic lateral resolution test device for imaging mass spectrometry. *Anal. Chem.* **2014**, *86*, 9473.
- [15] M. Pabst, S. R. Fagerer, R. Kohling, S. K. Kuster, R. Steinhoff, M. Badertscher, F. Wahl, P. S. Dittrich, K. Jefimovs, R. Zenobi. Self-aliquoting microarray plates for accurate quantitative matrix-assisted laser desorption/ionization mass spectrometry. *Anal. Chem.* **2013**, *85*, 9771.
- [16] P. L. Urban, K. Jefimovs, A. Amantonico, S. R. Fagerer, T. Schmid, S. Madler, J. Puigmarti-Luis, N. Goedecke, R. Zenobi. High-density micro-arrays for mass spectrometry. *Lab Chip* **2010**, *10*, 3206.
- [17] A. Zavalin, E. M. Todd, P. D. Rawhouser, J. Yang, J. L. Norris, R. M. Caprioli. Direct imaging of single cells and tissue at sub-cellular spatial resolution using transmission geometry MALDI MS. *J. Mass Spectrom.* **2012**, *47*, 1473.
- [18] P. Chaurand, K. E. Schriver, R. M. Caprioli. Instrument design and characterization for high resolution MALDI-MS imaging of tissue sections. *J. Mass Spectrom.* **2007**, *42*, 476.
- [19] S. Guenther, M. Koestler, O. Schulz, B. Spengler. Laser spot size and laser power dependence of ion formation in high resolution MALDI imaging. *Int. J. Mass Spectrom.* **2010**, *294*, 7.
- [20] A. Zavalin, J. Yang, R. Caprioli. Laser beam filtration for high spatial resolution MALDI imaging mass spectrometry. *J. Am. Soc. Mass Spectrom.* **2013**, *24*, 1153.
- [21] L. A. McDonnell, A. van Remoortere, R. J. van Zeijl, H. Dalebout, M. R. Bladergroen, A. M. Deelder. Automated imaging MS: Toward high throughput imaging mass spectrometry. *J. Proteomics* **2010**, *73*, 1279.

SUPPORTING INFORMATION

Additional supporting information may be found in the online version of this article at the publisher's website.